

Flat Cell Culturing Surface May Cause Misinterpretation of Cellular Uptake of Nanoparticles

Shahed Behzadi, Naazanene M. Vatan, Kevin Lema, Dike Nwaobasi, Ilia Zenkov, Parisa P. S. S. Abadi, Daid Ahmad Khan, Claudia Corbo, Haniyeh Aghaverdi, Omid C. Farokhzad,* and Morteza Mahmoudi*

In vitro cellular uptake of nanoparticles (NPs) is typically evaluated using a monolayer of cells seeded on a 2D culture plate, with the assumption of reliable and reproducible outcomes. However, recent developments reveal that 2D culture may produce errors in the measurement of cellular uptake of NPs due to issues including sedimentation and diffusion of NPs in cell-culture media. To shed more light on the effect of culture methods on the uptake of NPs, the same number of prostate cancer cells is cultured in 2D and 3D substrates and their uptake of quantum dots (QDs, as a model NP) and entrance mechanisms are assessed. Significantly fewer QDs are taken up, but they are more evenly distributed among the cells, in the 3D compared to the 2D culture method; in addition, QDs enter the cells via different mechanisms of endocytosis in 2D than they do in 3D approaches. Findings regarding cell cycle phase distribution also vary between 3D and 2D samples, which results in a significantly lower percentage of QDs being taken up in 3D compared to 2D culture. These findings indicate that the culture environment drastically influences NP–cell readouts, which may lead to misinterpretation of in vitro outcomes.

cell-culture platforms almost always show superior biological efficacy with NP-based drug delivery systems.^[2b,4] This consistent disparity in performance is attributed mainly to the inability of conventional 2D cell-culture method to replicate the 3D environment of tissues/tumors. Just one contributing factor is the lack of an extracellular barrier on the top side of the cell layer in the culture plate that the same cells would have in a 3D environment.^[5] Thus, while 2D cell culture allows NPs to reach their intended target easily by diffusing over a relatively short distance and binding to cells, the same NPs delivered in vivo are impeded by extracellular factors such as the densely packed cell clusters themselves and the relatively small pore sizes within the fibrillar collagen of extracellular matrix (ECM) and the tortuosity of the interstitial space.^[6]

1. Introduction

Nanoparticles (NPs) have gained increasing attention as carriers to deliver therapeutic agents into cancer cells by taking advantage of the enhanced permeation and retention effect.^[1] Monolayer 2D cell cultures are customarily used as an in vitro testing platform to evaluate the biological efficacy of NP-based drug-delivery systems.^[2] Although much of our basic understanding of NP-based drug delivery has been derived from the use of such platforms, conventional 2D cell culture does not adequately represent the in vivo scenario such as that offered by animal models.^[3] In fact, compared with in vivo conditions, 2D

Cell shape may also have a substantial influence on cellular uptake of NPs.^[7] Cells in 2D cultures are limited to a planar and spread morphology and do not assume the 3D morphologies of their native tissues.^[8] Another important variable is that the amount of cell membrane exposed to NPs depends significantly on whether the cells are cultured in 2D or 3D; NP internalization would be expected to vary accordingly. The extent to which cell shape is altered depends largely upon the stiffness of the culture substrate, which affects the biological activity of cells and their responses.^[9] For example, human mammary epithelial cells respond to matrix stiffness by altering their expression of at least 1500 genes spanning multiple functional categories.^[10] Cells in 2D monolayer cultures are generally exposed to a uniform and static medium with an elastic modulus (E) of 2–4 GPa, whereas cells in tissues are exposed to a dynamic environment with E ranging from 200 Pa (lung) to 18 kPa (prostate) to 18 GPa (cortical bone).^[11] Therefore, culturing all cells on the same substrate may yield misleading results, especially when the uptake of certain NPs into the cells is enhanced or repressed by one or more proteins whose expression on the cell membrane is dependent on stiffness.^[12]

The above factors have led to a growing interest in developing technologies to better mimic the 3D environment for screening NP uptake. Though the most realistic 3D model is almost

Dr. S. Behzadi, N. M. Vatan, K. Lema, D. Nwaobasi, I. Zenkov, Dr. P. P. S. S. Abadi, D. A. Khan, Dr. C. Corbo, Dr. H. Aghaverdi, Prof. O. C. Farokhzad, Dr. M. Mahmoudi
Center for Nanomedicine and Department of Anesthesiology
Brigham and Women's Hospital
Harvard Medical School
Boston, MA 02115, USA
E-mail: ofarokhzad@bwh.harvard.edu; mmahmoudi@bwh.harvard.edu

 The ORCID identification number(s) for the author(s) of this article can be found under <https://doi.org/10.1002/adbi.201800046>.

DOI: 10.1002/adbi.201800046

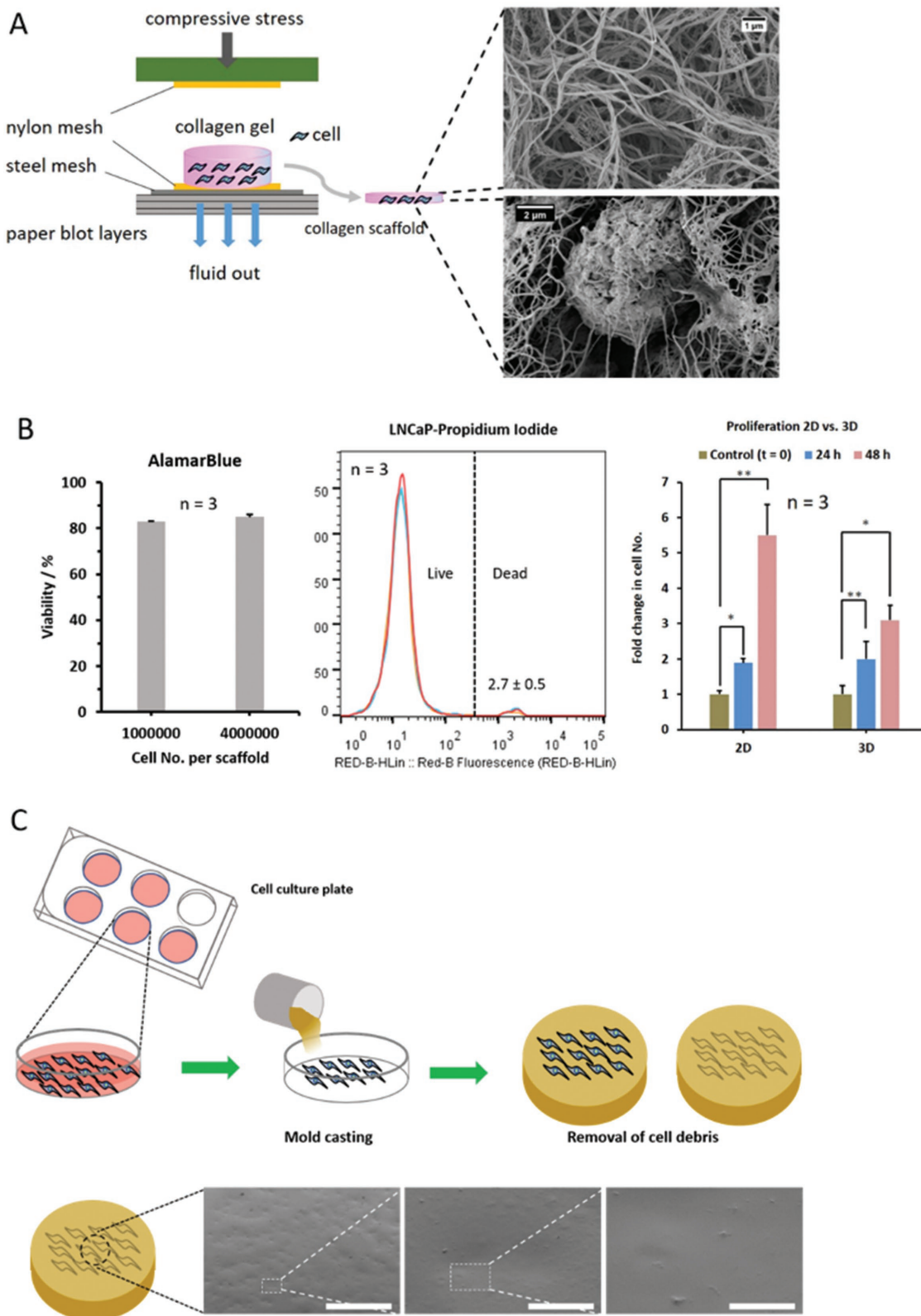


Figure 1. A) Schematic illustration of the collagen scaffold. Plastic compression of highly hydrated collagen gels was used to fabricate a dense fibrillar scaffold structure (i.e., collagen patch); the panel on the right shows scanning electron microscopy (SEM) of the collagen patch fibrillar ultrastructure with and without cells. B) AlamarBlue cell viability assay and flow cytometry for analysis of cell viability using propidium iodide for LNCaP cells embedded inside collagen scaffolds; proliferation assay for 2D and 3D cell-culture conditions at $t = 24$ and 48 h (two-tailed t -test results ($* = p < 0.005$))

certainly organ explant culture,^[13] it may not be the most practical, given the limited supply and the complexity of imaging and tracking NPs.^[3b] A popular current approach for 3D culture is suspending cells in liquid medium to form multicellular spheroids.^[14] However, although cell spheroids are the most convenient type of 3D culture in terms of preparation, limited spheroid size, heterogeneity of cell lineage, and lack of matrix interaction make them potentially unrealistic for the measurement of NP uptake.^[2b,15] Scaffolds are another type of 3D cell-culture system designed to bridge the gap between 2D and 3D cell culture.^[16] A customizable physical, mechanical, and biochemical environment as well as the ease of tracking NPs is among the advantages of scaffolds; however, possible batch variations, lack of transparency, changes in scaffold properties over time, and difficulties in sample harvesting for analysis have all been mentioned as challenges for investigating NP uptake.^[3b] Many microfluidics devices have been developed to study the biological behaviors of cells, tissues, and organs.^[2b,17] Despite the valuable insights for drug discovery offered by this technique,^[18] it remains skill intensive, limited in batch size, and requires the immobilization of cells. Additionally, microfluidics requires flow networks representative of in vivo microvascular beds and hydrogels sufficiently strong to withstand the stresses imparted by perfusion.^[19] Therefore, there is a strong need for a 3D cell-culture platform with high functionality to investigate NP uptake.

In this study, we show differences in cell–NP interactions between the conventional 2D model, a cell-imprinted model (which can give cells a 3D structure similar to the one they assume in their native tissues), and 3D collagen-fibrillar scaffolds (which enable high-density 3D culture). Here, we use commercially available quantum dots (QDs) as a model NP due to their ability to sustain fluorescence, their minimal cytotoxic effects on live cells, and their ability to yield reproducible results.^[20] In addition to the 3D model, we also employed a cell-imprinted substrate to allow the cells to take on their 3D shapes. We hypothesize that using the cell-imprinted substrate allows us to focus solely on the impact of cellular morphology on uptake. The 3D scaffolds are designed with an elastic modulus emulating the stiffness of a cancerous medial apex of the prostate ($E = 15$ kPa).^[21] LNCaP cells (a human prostate-cancer cell line) are used as the model system, and the scaffold is designed to mimic the tumor environment, e.g., cells are surrounded with collagen nanofibers imitating the ECM. In fact, our findings suggest that the effects of cell-culture environment on cell–NP interactions also need to be accounted for when studying NP uptake.

2. Results and Discussion

2.1. Biological Evaluation of 2D Cell Culture and 3D Cell-Laden Collagen Scaffolds

3D collagen nanofibrillar scaffolds embedded with LNCaP cells were intended to encourage more-complex cellular organization

and to provide environmental stiffness close to cells' residential tumor microenvironment (i.e., the cancerous medial apex of the prostate region, where $E = 15$ kPa).^[21] In the 3D culture system, cells' native tissue memory may be invoked by allowing them to self-assemble and re-orient in their own native spatial arrangement. Moreover, 3D culture substrates encourage cells to form more realistic in vivo like cell–cell interactions. Furthermore, in 3D cell models, the appropriate ECM layer (i.e., collagen fibers) and the densely packed cell clusters simulate a more-realistic mass transfer gradient than would be possible in 2D.^[3a,5,6]

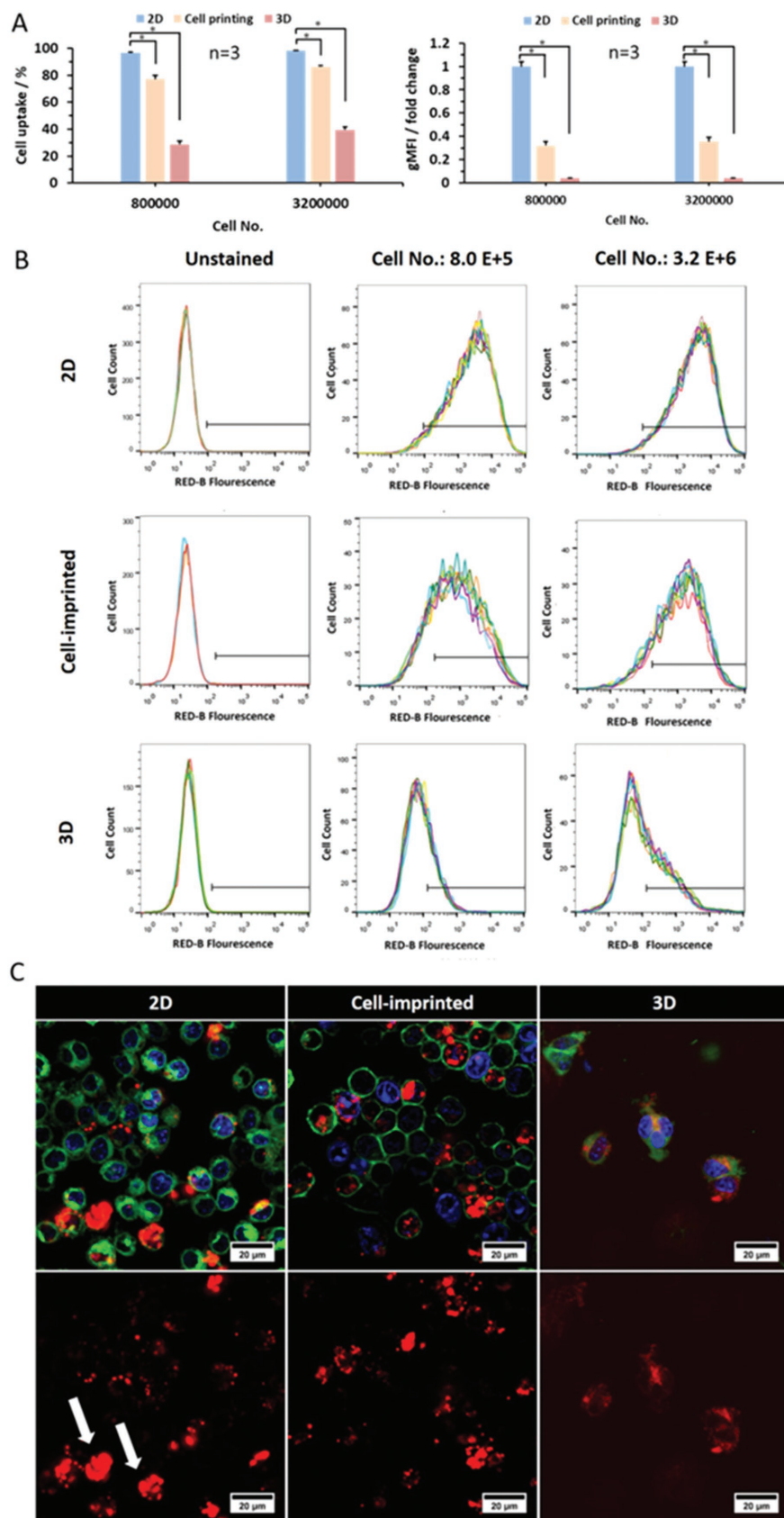
Plastic compression of highly hydrated collagen gels was used to fabricate a dense fibrillar scaffold structure (Figure 1A).^[22] To ensure that cells cultured in the 3D environment were alive and healthy after compression, cell viability was measured and compared with that of cells cultured in the 2D plate. Results indicated that cells retained their metabolic activity and membrane integrity following scaffold preparation (Figure 1B). Furthermore, cell counts showed that 2D and 3D cultured cells underwent similar fold changes in proliferation after 24 h (Figure 1B). However, after 48 h, the change in 2D cell number increased dramatically beyond the growth exhibited in the 3D scaffolds (Figure 1B).

2.2. Effects of Morphology of Cell Culturing Substrate on the Uptake of QDs

To analyze the uptake of QDs, LNCaP cells were cultured in three different cell-culture environments: (i) 2D conventional polystyrene culture plate, (ii) cell-imprinted substrate having multiscale features of LNCaP cells (where the same type of cells were used to make a template for the fabrication of the substrates; see Figure 1C for details), and (iii) 3D collagen nanofibrillar patches, by which cells are embedded and distributed inside the scaffolds (i.e., semi-in vivo conditions; see Figure 1C).

To assess the intracellular accumulation of QDs, we calculated the percentage of cells in which NP uptake occurred (uptake%) and geometric mean fluorescence intensity (gMFI) values from flow cytometry, which indicate the mean number of NPs taken up per cell. After dissolving the collagen scaffolds, the number of cells embedded in the scaffolds was counted and the same number of cells (i.e., 8×10^5 and 3.2×10^6) was seeded on the cell-culture plate and cell-imprinted substrates. The 2D cell-culture plate with cell density 8×10^5 had cellular uptake of 96%, while QDs entered only 77% of cells seeded on cell-imprinted substrate. For 3D culture, uptake percentage was dramatically lower: 28%. We also performed the same experiment with a higher cell density (3.2×10^6) but the same NP-to-cell ratio, a factor thought to affect cell–cell interactions and cell cycle phase distribution and, consequently, NP uptake.^[23] While an increase in density did not affect NP uptake by 2D-cultured cells, NP uptake increased to 86% and 40% for cell-imprinted substrate and 3D collagen scaffolds, respectively.

and (** = $p < 0.05$), sample size ($n = 3$). C) Schematic illustration of cell-imprinting method; cells were seeded on a polystyrene culture plate and their morphologies transferred to a silicone replica by mold casting. After a curing step, the cell debris was removed and the silicone cast acted as a negative replica with an imprinted pattern of the cell surfaces. SEM images show the morphology obtained on the cell-imprinted replicas for LNCaP cells (tilt angle: 45°; magnification (left to right): 200, 2k, 10k; scale bar (left to right): 500, 50, and 10 μm).



The same trends were observed for gMFI, i.e., mean number of NPs taken up per cell. The highest intensity was in 2D-cultured cells, followed by cell-imprinted substrate, and finally 3D culture. Although the cell-printed samples exhibited a 20% lower uptake than 2D-cultured cells, gMFI decreased more drastically, by threefold. This was also observed with 3D-cultured cells, which showed a 70% lower uptake and 25-fold lower gMFI (Figure 2A,B).

In 2D-cultured cells, the distribution of QDs taken up (arrows in Figure 2C) was irregular among cells, i.e., some cells took up significantly more QDs than others. This could be due to sedimentation and diffusion of the QDs on the 2D culture plates, as shown previously.^[24] For cell-printed samples, the accumulation of QDs taken up per cell was more balanced, although several aggregates were identified. Conversely, in 3D-cultured samples, QDs accumulated very evenly among the cells, with no large aggregates.

After endocytosis, NPs are exposed to a range of pH levels (4.5–6.0) within different cellular compartments.^[25] At pH values of 5 and lower, the stability of QDs decreases causing them to aggregate, which results in a lower fluorescence intensity.^[25,26] This leads us to predict that the difference of gMFI between 2D and 3D would be even greater, as our results show that QDs taken up in 2D cultured cells are more aggregated as compared to 3D-cultured cells.

Figure 2. Uptake of red-fluorescent quantum dots (QDs) and ranking of the concentration of QDs in the cells. LNCaP cells were exposed to QDs (concentration = 1×10^{-9} M and volume = 2 mL RPMI-1640 containing 10% FBS) for 2 h before flow cytometry measurements and imaging. A) The uptake of QDs and geometric mean fluorescence intensity (gMFI) of QDs in the cells were evaluated by flow cytometry. gMFI for cell-imprinted substrate and 3D cell culture were normalized to the 2D cell culture. B) Flow cytometry distributions of cell fluorescence intensity after 2 h exposure to NPs for cells cultured in 2D cell culture, cell-imprinted substrate, and 3D cell culture at two different cell densities (i.e., 8.0×10^5 and 3.2×10^6). C) Confocal images after 2 h exposure show NP accumulation and distribution in the cells. Blue, nuclei (DAPI); green, plasma membrane (FITC); red, red-fluorescent QDs (* = $p < 1.0 \times 10^{-5}$ by two-tailed *t*-test compared to control, sample size (n) = 3).

2.3. Effects of Morphology of Cell Culturing Substrate on the Endocytic Pathways of QDs

Cells may take up QDs through several different mechanisms, which fall into five main types of endocytosis: phagocytosis, caveolin-mediated endocytosis, clathrin-mediated endocytosis, clathrin/caveolae-independent endocytosis, and micropinocytosis.^[27] To investigate whether 2D and 3D culture of cells can alter the mechanism of uptake, we evaluated six potential endocytic inhibitors for 2D and 3D cell-culture conditions. We selected the endosome interfering reagent bafilomycin A1 (BAF), the caveolae-mediated endocytic inhibitor filipin III, the clathrin-mediated inhibitor chlorpromazine (CPZ), the macro-pinocytotic inhibitor 5-(*N*-ethyl-*N*-isopropyl)-amiloride (EIPA), the inhibitor of F-actin assembly cytochalasin D (CytD), and the inhibitor of phospholipase C (i.e., downstream of G-protein coupled receptor associated pathway) U-73122. AlamarBlue viability assays at multiple concentrations of the inhibitors for the 2D cell-culture condition (Figure S1, Supporting Information) showed that the inhibitors were not toxic to the cells at any concentration assessed, except for U-73122 at the concentration of 4 $\mu\text{g mL}^{-1}$, where viability decreased to 55% (Figure S1, Supporting Information). For 2D-cultured cells, three concentrations of each inhibitor were tested for uptake by flow cytometry (Figure S2a, Supporting Information). Results varied greatly among the inhibitors tested (Figure S2a,b, Supporting Information). For U-73122, both uptake percentage and gMFI remained almost unaffected at concentrations below 4 $\mu\text{g mL}^{-1}$. At 4 $\mu\text{g mL}^{-1}$ U-73122, uptake dropped to 76%, and gMFI dropped by twofold, which might be attributed to toxicity. While uptake percentage remained the same in the case of CytD, addition of the inhibitor raised fluorescence intensity 1.5-fold, indicating an increase in QDs per cell. In cells incubated with filipin III, inhibitors at all concentrations saw a marginal decrease in uptake, with no notable differences in gMFI. The only notable change produced by incubation with CPZ, a 1.5-fold increase in gMFI, occurred at the highest inhibitor concentration—but uptake percentage remained unaffected in all three cases. Cells incubated with either EIPA or BAF were completely unhindered, as there was no significant difference in uptake or gMFI. For cells grown in the 2D model, uptake data following incubation with inhibitors proved to be non-reproducible, despite replication of experimental conditions. As shown in Figure S2b (Supporting Information), histograms were inconsistent, as data underwent curve shifts.

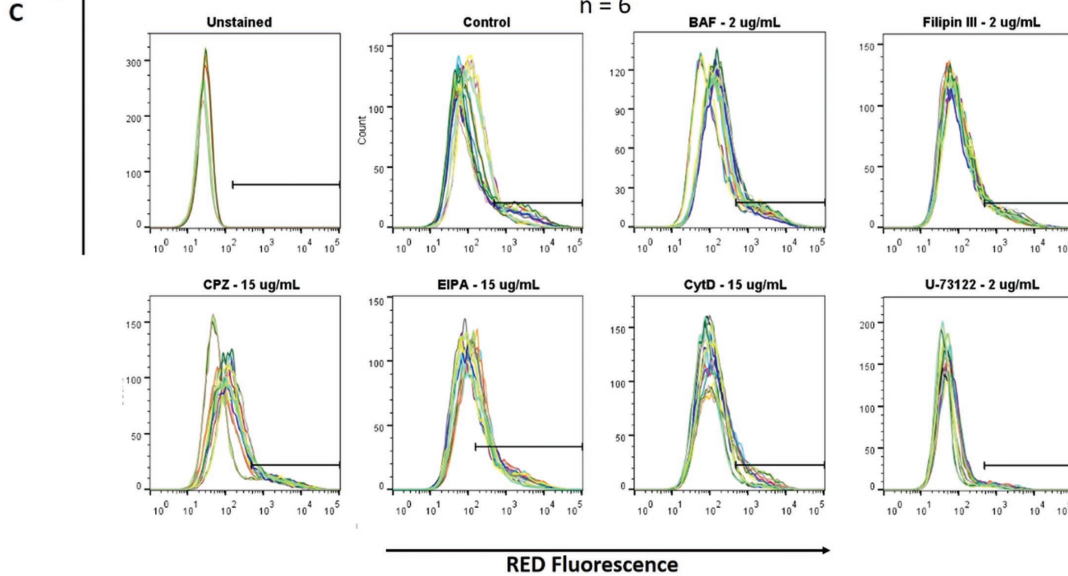
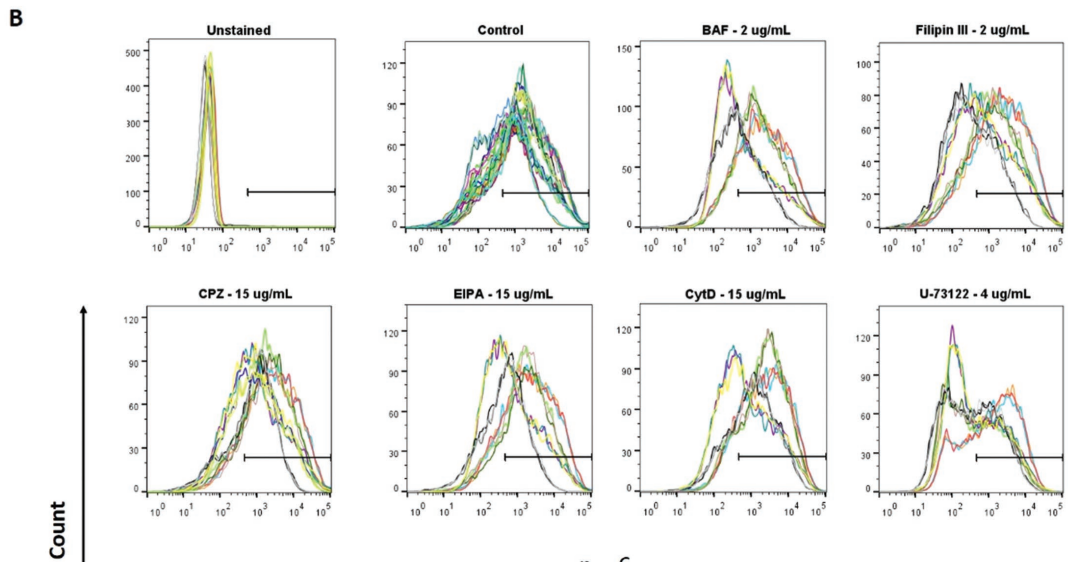
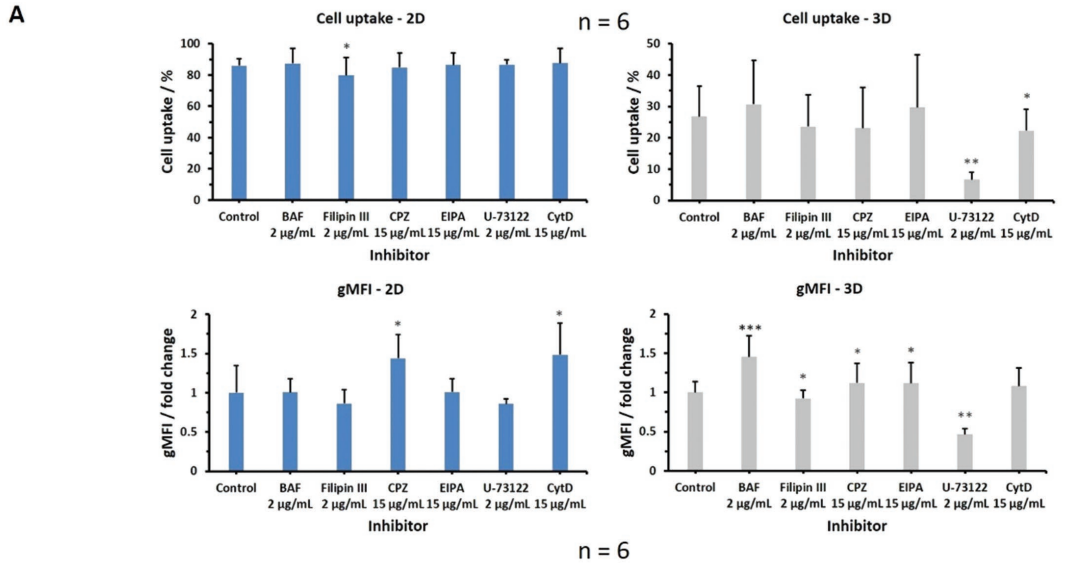
The highest tested concentration for each inhibitor, except for U-73122, was used for uptake measurements in 3D cell culture. At the concentrations used, inhibitors did not cause a significant difference in uptake percentage in 3D cultured cells (Figure 3A,B); except for U-73122 (2 $\mu\text{g mL}^{-1}$) and CytD (15 $\mu\text{g mL}^{-1}$), which caused reductions in uptake percentage of 7% and 22%, respectively. However, incubating cells with an inhibitor led to a significant difference in gMFI in most cases. Incubation with BAF, CPZ, or EIPA resulted in higher fluorescence intensities for 3D cells. 2D cells also experienced gains ($\approx 10\%$) in intensity following incubation with CPZ and CytD. It is increasingly being understood that these chemical inhibitors are not highly specific and their efficacy is dependent on the cell line.^[28] By suppressing certain

uptake pathways, these inhibitors may have upregulated other mechanisms.^[28] CytD has previously been shown to slightly increase the uptake of QDs in human epidermal keratinocytes (HEKs).^[25] Previously, it was shown that incubation with CPZ led to an increase in the uptake of holo-transferrin and lactosylceramide in certain cell lines.^[28] A possible reason could be that CPZ being an amphipathic molecule integrates into cell membrane and increases its fluidity, resulting in a higher uptake.^[29] Addition of U-73122 induced a twofold decrease in gMFI in the 3D cell model; filipin III also caused a 10% reduction (histograms in Figure 3B,C). Uptake measurements were erratic for 2D-cultured cells, as distribution changed quite dramatically from trial to trial. Although experimental conditions were kept the same, less-reproducible results were obtained for 2D-cultured cells than for 3D cells, which in contrast produced consistent results for all inhibitors (Figure 3B). Several studies have shown that the mechanism of action of QDs (e.g., toxicity) depends on multiple factors derived from both physicochemical properties and environmental conditions.^[30] In a previous study, it was found that the G-protein-coupled receptor-associated pathway regulates the uptake of QDs in HEKs.^[25] However, when we inhibited this uptake pathway, we observed no significant decrease in NP uptake for LNCaP cells seeded in 2D culture plates. This could be attributed to either environmental conditions or the cell type, as it has been reported that NP uptake mechanisms can differ significantly among cell lines.^[31]

Viability assays using AlamarBlue revealed that all of the inhibitors tested showed no cytotoxicity to the cells except U-73122. To further understand the effect of U-73122 on metabolic activity, cell viability was measured in both 2D and 3D cultures at 4 and 8 h, as it had induced the strongest inhibitory effects during the previous uptake experiment (Figure S3, Supporting Information). After 4 h of incubation, 2D cells exhibited significant reductions in viability at all three tested inhibitor concentrations: 1, 2, and 4 $\mu\text{g mL}^{-1}$ of U-73122 resulted in drops of 18%, 20%, and 27%, respectively. For the 3D model, cells incubated with 4 $\mu\text{g mL}^{-1}$ of the inhibitor experienced a significant drop in viability, falling by 20%. Moreover, 2D cells incubated for 8 h with U-73122 at concentrations of 1, 2, and 4 $\mu\text{g mL}^{-1}$ demonstrated significant drops in viability of 16%, 30%, and 47%, respectively. Again, in the case of 3D cultures, the only cells to undergo a notable drop in viability were those incubated at 4 $\mu\text{g mL}^{-1}$, which exhibited a 22% decrease.

2.4. Effects of Cell Cycle on the Uptake of QDs for 2D and 3D Cell-Culture Conditions

A previous study reported that cell-cycle phase plays a critical role in the uptake of NPs.^[23] In fact, the accumulation of NPs in cells could be ordered according to phase: G0/G1 < S < G2/M. Phase distribution was found to differ between 2D and 3D culture conditions (Figure 4A). Motivated by this finding, we sought to examine NP uptake in both 2D and 3D with synchronized cell-cycle phase distributions. Fetal bovine serum (FBS) starvation was implemented to arrest and synchronize the 2D and 3D cells, and phase percentage was determined using propidium iodide (PI) guided flow cytometry. Starvation



was effective in synchronizing the 2D and 3D cells (Figure 4A and Figure S4, Supporting Information). Upon confirmation of phase synchronization for cells cultured in 2D and 3D conditions, uptake percentage and gMFI were measured. In the case of 2D-cultured cells, uptake percentage changed very little (Figure 4B), with samples sustaining a drop of only 5% in uptake as a result of the 20% increment in G0/G1 cells. However, gMFI decreased twofold compared to control cells (Figure 4B). The pronounced drop in NP uptake was attributed to cell size, since it has been reported that quantity of NPs taken up per cell is dependent on size.^[7] For cells at different phases in the cell cycle, G2 take in the most NPs, followed by S, and finally G0/G1. These differences in uptake do reflect cell size, which increases as cells approach the M phase. Thus, the increase in the G0/G1 population accounts for the decline in NP uptake. Consistent with previous reports, increasing the population of G0/G1 cells produced a significantly smaller cell area (i.e., 20%), an average reduction of 80 μm (Figure 4C).^[7] Furthermore, uptake percentage dropped more dramatically (by 66%) in 3D serum-starved cells in comparison to 3D controls. Additionally, fluorescence intensity dropped almost threefold. However, the most noteworthy result is that uptake percentage in 3D cells was 80% lower than in 2D cells. This indicates that when cell phase is synchronized, the difference in cellular uptake between 2D and 3D models is greater than previously assumed.

2.5. Effects of Sedimentation on the Uptake of QDs

Even dispersion of NPs via cellular uptake has been reported to be hindered by particle sedimentation and diffusion.^[24] In some circumstances, particles can aggregate and sediment very quickly, leading to a concentration at the monolayer surface higher than the initial particle dose, which results in profound effects on cellular uptake.^[24] In fact, previous research has shown that cellular uptake is independent of parameters such as size and shape, depending instead on sedimentation and diffusion velocities.^[24] Those sprang from comparison of the uptake of gold NPs in typical 2D cultured cells with a 2D inverted configuration. Similarly, we analyzed NP uptake in 2D, 2D inverted, and 3D cells. Those findings allowed us to exclude the sedimentation effect, yielding a more-accurate comparison of 2D and 3D model uptake.

To investigate the effect of sedimentation, the 2D culture experiment was replicated using QDs (Figure 5A). Cells were grown on glass cover slides and inverted prior to QD exposure using specially designed holders. Samples were then incubated with QDs and analyzed via flow cytometry. Inversion reduced uptake percentage to 88% (Figure 5B and Figure S5, Supporting Information) as well as eliciting a staggering fivefold drop in gMFI. Confocal microscopy

(Figure 5C) confirmed these results. 2D control samples exhibited extensive uptake and aggregation. Conversely, uptake in inverted cell samples was far more modest, with very few particles taken up per cell. Despite the decrease, inverted 2D cells exhibited almost threefold higher uptake than 3D cells (i.e., 88% vs 28%) and fourfold higher gMFI (i.e., 18% vs 3.7%). This indicates that even when accounting for the effect of sedimentation, the 2D model still significantly overestimates NP uptake.

3. Conclusions

Our results show conclusively that the choice of cell model, whether 2D or 3D, significantly affects the uptake of NPs. Cell populations grown in 2D culture plates consistently demonstrated greater overall uptake percentage and NPs taken up per cell compared to those grown in 3D cell scaffolds. Morphologically, 2D cells differed from their 3D counterparts in part due to the high area of contact with the plastic surfaces of culture vessels. While cells grown in a 3D scaffold retain their native shape and spatial arrangement, 2D-cultured cells flatten out on the bottom of the petri dish. Endocytic inhibitors induced differences in uptake between the two cell models. After exposure to certain inhibitors, fluorescence intensity revealed significant increases in 3D cells that were absent in 2D. This may indicate that the more “realistic” cellular matrix of the 3D scaffold allowed the inhibitors to alter the mechanism and pathway of NP uptake. Cell cycle should also be considered in cellular uptake studies. We found that cycle synchronization significantly affects uptake in 2D and 3D models, but to different extents. In addition to morphology, cell configuration also played a key role in the uptake of NPs. For control 2D-cultured cells, QDs were found to sediment, leading to high levels of measured uptake and gMFI. This was supported by the finding in 2D inverted cells that uptake was significantly reduced. Nonetheless, uptake percentage and gMFI in 2D were still twofold higher than in the 3D scaffold, even with the exclusion of sedimentation. Differences in cellular uptake attributable to several parameters including cell shape, matrix/substrate stiffness, NPs’ aggregation, sedimentation, and diffusion. Further work is necessary to determine the contribution of each of the factors toward cellular uptake of NPs. Therefore, the culture model should be carefully considered and reported in future publications.

4. Experimental Section

Cell Preparation: LNCaP cells were directly purchased from ATCC and cultured in RPMI-1640 medium (Hyclone, UT, US) with 10% FBS (Hyclone, UT, US) and 1% pen/strep (Anti-Anti, Gibco, US).

Figure 3. A) Uptake of red-fluorescent quantum dots (QDs) and geometric mean fluorescence intensity (gMFI) in LNCaP cells either seeded on a polystyrene culture plate (i.e., 2D condition) or embedded in collagen scaffold after 1 h incubation with inhibitors were evaluated by flow cytometry. (bafilomycin A1 (BAF): 2 $\mu\text{g mL}^{-1}$; filipin III: 2 $\mu\text{g mL}^{-1}$; chlorpromazine (CPZ): 15 $\mu\text{g mL}^{-1}$; 5-(N-ethyl-N-isopropyl)-amiloride (EIPA): 15 $\mu\text{g mL}^{-1}$; U-73122: 1, 2, and 4 $\mu\text{g mL}^{-1}$; cytochalasin D (CytD): 15 $\mu\text{g mL}^{-1}$). Flow cytometry distributions of cell fluorescence intensity after 2 h exposure to QDs for cells cultured in either B) 2D or C) 3D cell culture in the presence of the inhibitors prior to uptake experiments (* = $p < 0.05$, ** = $p < 1.0 \text{ E-}7$, and *** = $p < 1.0 \text{ E-}18$ by two-tailed *t*-test compared to control, sample size (n) = 6).

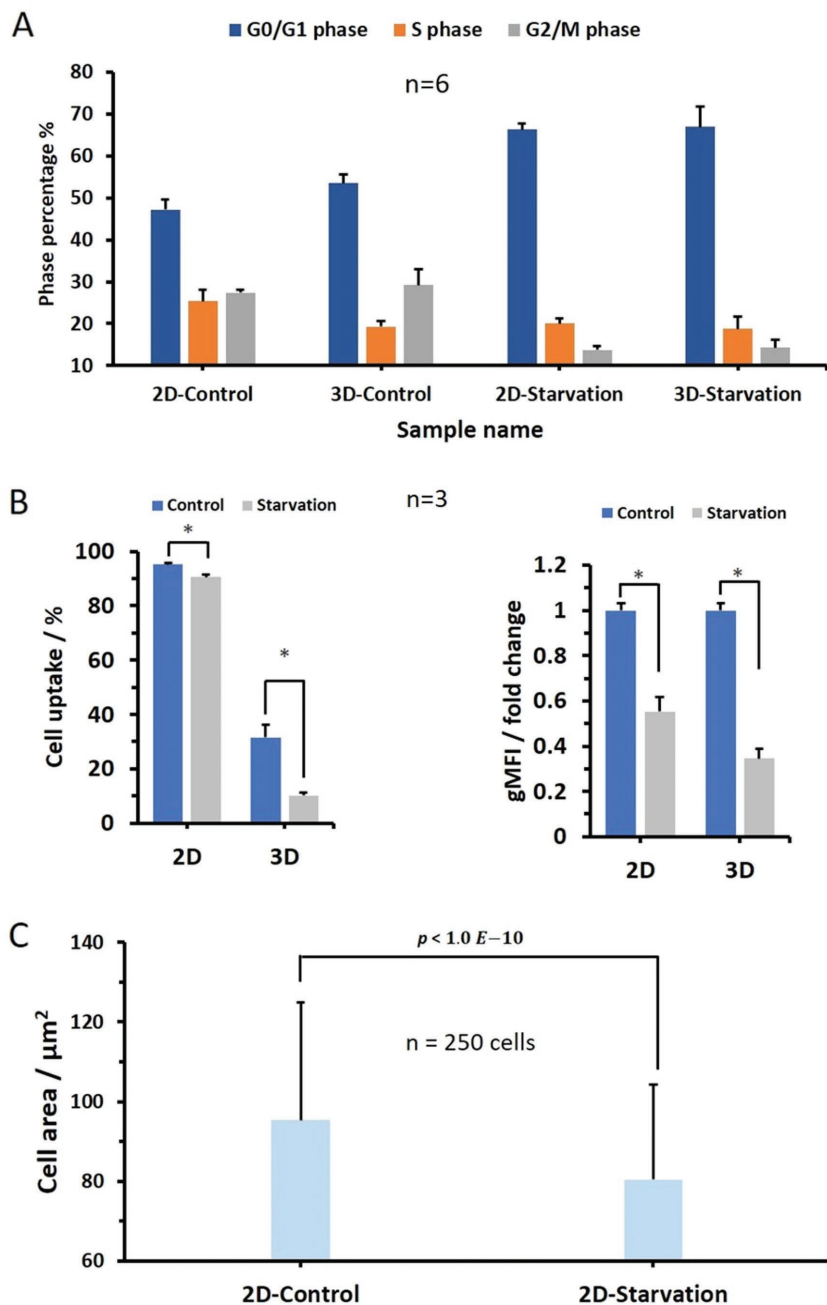


Figure 4. The cell cycle and its role in NP uptake. To synchronize LNCaP cells in 2D and 3D conditions, cells were serum starved for 42 h prior to uptake experiments. A) Comparison of cell cycle analysis of serum-starved cells and controls for both 2D and 3D conditions, showing percentages of G0/G1 phase, S phase, and G2/M phase of serum-starved and control cells (sample size (n) = 6). B) Uptake of QDs and geometric mean fluorescence intensity (gMFI) in LNCaP cells cultured in either 2D or 3D conditions ($*$ = $p < 1.0 \text{ E-}5$ by two-tailed t -test compared to control, sample size (n) = 3). C) Cell area of LNCaP cells cultured in 2D conditions under normal and serum-starved conditions for 42 h. Cell area was calculated using Image J for 250 cells in both conditions (sample size (n) = 250 cells).

Fabrication of Cell-Imprinted Substrate: LNCaP cells were seeded in 6-well plates at either 8×10^5 or 3.2×10^6 cells per well. The plates were kept for 24 h in the relevant cell-culture medium supplemented with 10% FBS and 1% pen/strep in an incubator. For the fabrication of cell-imprinted substrates, polydimethylsiloxane (Sylgard 184, RTV, Dow

Corning) was used. The silicone resin and curing agent were mixed at a ratio of 10:1 w/w and kept under vacuum for 1 h at room temperature. The cell-culture medium was removed, and cells were rinsed and fixed with phosphate buffered saline (PBS) 1X and 4% paraformaldehyde (PFA) solution in PBS 1X, respectively. After removing the fixation solution, the surface of each well was covered with a layer of elastomer (≈ 2 mm) and the plate was kept at 37 °C overnight. The cured silicone was peeled off the cell-culture plates and extensively washed using 1 M NaOH solution to remove remaining cells and other chemicals. The resulting cell-imprinted substrates were placed in 6-well plates and the relevant cells seeded at either 8×10^5 and 3.2×10^6 cells per well in the appropriate cell-culture medium, supplemented with 10% FBS and 1% pen/strep. Figure 1 presents the scheme of cell imprinting.

Formation of Cellular Compressed Collagen Gel (i.e., Collagen Scaffold): To fabricate collagen scaffolds containing LNCaP cells, the RPMI-1640 culture medium (Hyclone, UT, US) was removed via centrifugation, and the LNCaP cell pellet re-dispersed in 1.1 mL 1X Dulbecco's modified Eagle's medium (DMEM) (Hyclone, UT, US). The resulting LNCaP cells-DMEM was mixed with 0.9 mL sterile rat tail type I collagen solution in acetic acid (3.84 mg mL, Millipore, MA, US) and neutralized with 0.1 M NaOH (Sigma-Aldrich) ($\approx 55 \mu\text{L}$). The collagen solution (1 mL) was distributed into 24-well plates (15.6 mm in diameter) and placed in a tissue culture incubator for 30 min at 37 °C for collagen gel polymerization. Collagen gels were then compacted by application of a static compressive stress of ≈ 1400 Pa for 3 min (see ref. [22] for details), eliciting 98–99% volume reduction (Figure 1).

Nanoparticle Uptake: To measure QD (Qtracker 655 Cell Labeling Kit, Invitrogen, US) uptake in a 2D environment, cells were seeded in 6-well plates at a density of 8×10^5 cells per well. Cells were kept in 2 mL of the relevant medium with 10% FBS and incubated overnight at 37 °C in 5% CO_2 . The cells were then incubated in 1 mL of FBS-free medium for an additional 30 min. To prepare 1×10^{-9} M QDs, 1 μL each of Qtracker Component A and Component B was mixed in a 1.5 mL microcentrifuge tube and kept for 5 min at room temperature. Two milliliters of fresh growth medium containing 10% FBS was added to the tube and vortexed for 30 s. Cells (either 2D or 3D) were incubated with QD solution and given 2 h in the incubator to take up the QDs. For the 2D condition, each well was washed twice with 2 mL of PBS, and cells were detached using 0.25% trypsin (Corning, US). Cells were then spun down and re-suspended in 4% PFA in PBS. After 30 min in the incubator, cells were once again spun down and re-suspended in PBS. For the 3D condition, 2 mL of RPMI-1640 with 10% FBS containing 6 mg of collagenase from *Clostridium histolyticum* (Sigma, US) was used to break the peptide bonds in collagen scaffolds. Samples were transferred into a 96-well plate and analyzed via the Guava easyCyte flow cytometer with 10 000 cells gated on the basis of forward and side scatter. A 488 nm laser was used to excite the QDs and the data were stored and processed using FlowJo_V10 software. An unstained sample (i.e., no QDs) was used to determine the gate. Different preparation methods were applied for flow cytometry for 2D and 3D samples following NP uptake. For 2D, trypsin was used to detach

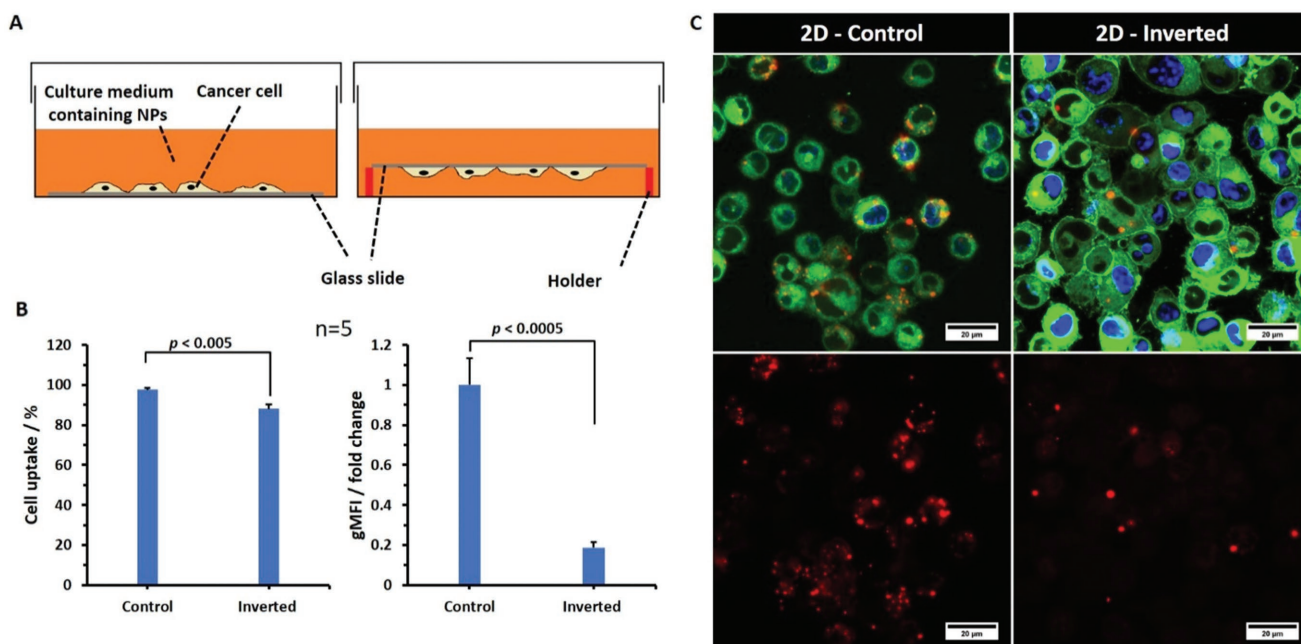


Figure 5. A) Schematic of upright (left) and inverted (right) configurations for measuring cellular uptake of QDs. B) Uptake of QDs and ranking of the concentration of QDs in the cells seeded on cell-culture well plates and cover slides under 2D conditions (cellular uptake%: $p < 5.0 \times 10^{-3}$, gMFI: $p < 5.0 \times 10^{-4}$, by two-tailed *t*-test compared to control, sample size (n) = 5). C) Confocal images after 2 h of exposure show QD accumulation and distribution in the cells. Blue, nuclei (DAPI); green, plasma membrane (FITC); red, red-fluorescent QDs.

the cells. It was speculated that trypsin may cleave NPs bound to the surface of 2D cells. To investigate whether trypsin's degradative effects influence the measurement of NP uptake, the concentration of NPs in the supernatant was measured after addition of trypsin. Its contribution was less than 1% of NP uptake. For the 3D scaffold, collagenase was used to dissolve the cell-laden patches post-NP incubation. 2D cells were incubated with a collagenase solution after NP uptake to determine whether it caused any change in fluorescence activated cell sorting (FACS) measurement, but no significant change was detected in the uptake of NPs (Figure S6, Supporting Information).

AlamarBlue Assay—(A) Cell Viability in Scaffolds: Collagen scaffolds containing LNCaP with 1.0×10^6 cells were prepared and kept in an incubator at 37 °C overnight. Two milliliters of the relevant medium containing 6 mg collagenase from *C. histolyticum* (Sigma, US) was used to break the peptide bonds in collagen scaffolds. Cells were collected and washed by adding 2 mL PBS 1X (Hyclone, US), centrifuging at $125 \times g$ for 10 min, and then decanting the supernatant from the pelleted cells. Cells were re-suspended in the relevant medium containing 10% FBS (Hyclone, US), counted, and seeded in a 96-well plate (Flat Bottom Black, Clear Bottom, Corning, US) ($100 \mu\text{L}$ at 1.0×10^6 cells per milliliter concentration) for 6 h at 37 °C and 5% CO_2 before proceeding with the assay. To include appropriate assay controls, cells in a cell-culture flask were collected, washed, and seeded into the 96-well plate at the same cell concentration (1.0×10^6 cells per milliliter). An amount of 10 μL of AlamarBlue reagent (Invitrogen, US) was directly added to cells in the 96-well plate. Absorbance at wavelengths of 570 and 600 nm (as a reference) was measured after 6 h. The percent difference in reduction between treated and control cells in cytotoxicity/proliferation assays was calculated. The results represent data from three independent experiments with statistics for five replicates.

AlamarBlue Assay—(B) Toxicity of the Inhibitors: The cytotoxicity of the inhibitors on LNCaP cells was evaluated for both 2D and 3D conditions using the AlamarBlue cell viability assay. For the 2D model, 6-well plates were seeded at an initial cell density of 8×10^5 cells per well. For the 3D model, collagen scaffolds were prepared with an initial cell density

of 1.0×10^6 cells per scaffold to account for the 80% encapsulation efficiency. Cells in both 2D and 3D environments were kept in 2 mL of medium with 10% FBS in an incubator (37 °C, 5% CO_2) overnight. Cells were then further incubated in 1 mL of FBS-free medium for an additional 1 h. Inhibitor solutions were prepared for the uptake assay, and cells were kept in 1.8 mL of FBS-free medium containing inhibitors for 1 h. Then 200 μL of FBS was added to each well, followed by 200 μL of AlamarBlue. After 2 h, 200 μL of each sample was transferred into a Costar flat transparent 96-well plate, and cell viability was measured with a Biotech Synergy plate reader. Measurements were taken 2, 4, and 8 h after AlamarBlue was added. To include appropriate assay controls for 2D conditions, cells were seeded in a 9-well plate with the same cell concentration (1.0×10^6 cells per milliliter), and for 3D conditions, collagen scaffolds were prepared with an initial cell density of 1.0×10^6 cells per scaffold. The results represent data from four independent experiments with statistics for three replicates.

Analysis of Cell Viability Using PI by Flow Cytometry: An amount of 2 mL of the relevant medium containing 6 mg of collagenase from *C. histolyticum* (Sigma, US) was used to break the peptide bonds in collagen scaffolds. Cells were collected and washed twice with 2 mL of PBS 1X (Hyclone, US), centrifuged at $125 \times g$ for 10 min, and then the supernatant was decanted from the pelleted cells. Cells were re-suspended in a flow-cytometry staining buffer (eBioscience, US) at a concentration of 1.0×10^6 cells per milliliter. PI staining solution (5 μL , 10 $\mu\text{g mL}^{-1}$) (Invitrogen, US) was added to 200 μL of each sample of otherwise unstained cells just prior to analysis and mixed gently.

Endocytic Mechanism Studies: LNCaP cells were seeded in 6-well plates at 1.0×10^6 cells per well. The endocytic inhibitors CytD (5, 10, and 15 $\mu\text{g mL}^{-1}$), CPZ (5, 10, and 15 $\mu\text{g mL}^{-1}$), U-73122 (1, 2, and 4 $\mu\text{g mL}^{-1}$), filipin III (0.5, 1, and 2 $\mu\text{g mL}^{-1}$), filipin III (EIPA 5, 10, and 15 $\mu\text{g mL}^{-1}$), and BAF (0.5, 1, and 2 $\mu\text{g mL}^{-1}$) were purchased from Cayman Chemical. The doses chosen were nontoxic to LNCaP cells (Figure S1, Supporting Information). LNCaP cells were washed with RPMI-1640 and serum starved for 1 h before incubation with inhibitors, which must be taken up by the cell before they can exert their effect. Each endocytic inhibitor (1 mL) was pre-dosed in the cell culture for 1 h

in triplicate wells and then dosed with 1 mL of the medium with 20% FBS containing QDs with or without inhibitors for another 2 h (total volume = 2 mL with 10% FBS). Cells were gently rinsed, detached, centrifuged, and re-suspended in 4% paraformaldehyde (Alfa Aesar, US) solution in PBS for 30 min in incubator. Cells were kept in a cold room (4 °C) until flow cytometry.

Culture Synchronization: To obtain G0/G1-cell-enriched cultures, plates were washed three times with PBS and incubated in 0.1% FBS regular medium for 48 h. To compare uptake in synchronized versus nonsynchronized culture, care was taken to ensure a similar number of cells (by cell counting after 48 h of starvation) and preparing the nonsynchronized cultures with the same number of cells. G0/G1 enrichment was analyzed using a cell cycle staining reagent (0.1% Triton X-100, Thermo Scientific, US) in 1X PBS containing 2% v/v% of 10 mg mL⁻¹ DNase-free RNase (Invitrogen, US) and 2.5% v/v% of 1 mg mL⁻¹ propidium iodide (Invitrogen, US) and flow cytometry after cell fixation with 70% ice-cold ethanol (VWR, US). To measure NP uptake in the G0/G1-enriched cultures, 0.1% FBS regular medium was first replaced by fresh medium with 10% FBS for 2 h to reduce starvation effects, and only then the cells were exposed to QDs.

Scanning Electron Microscopy: The nanostructure of the collagen with and without cells was analyzed using scanning electron microscopy (SEM) at 1–2 kV, using InLens SE detection. Collagen scaffolds were fixed by immersion in 4% paraformaldehyde solution overnight and washed twice with 0.1 M sodium cacodylate buffer (pH 7.4) and then postfixed in 1% aqueous osmium tetroxide (OsO₄) for 1 h. Samples were then washed twice in purified water and dehydrated in an increasing ethanol solution series (50%, 70%, 90%, and 100%, 2 × 15 min each). Finally, the specimens were critical-point dried (CPD) in liquid CO₂, in a Tousimis 815B critical-point dryer (Tousimis, MD). CPD-dried samples were mounted on standard SEM stubs with adhesive copper tape and sputter-coated with 4 nm of Au/Pd in a Denton Desk II machine (Denton Vacuum, NJ). Imprinted substrates were also carbon coated prior to imaging.

Statistical Analysis: The gMFI data for the control were normalized to 1 and gMFI data for test groups were normalized to the control. Mean and standard deviation are plotted as bar graphs for each group (sample size (*n*) ≥ 3). Two-tailed *t*-test (MS Excel) was used to determine the statistical significance of the data, with an alpha value of 0.05. Statistically different groups are marked with an asterisk and *p*-values are mentioned in the figure captions.

Supporting Information

Supporting Information is available from the Wiley Online Library or from the author.

Acknowledgements

The authors gratefully acknowledge funding from the US National Institutes of Health (NIH) grants HL127464-01A1 and EB015419 (to OCF) and the Department of Defense grant PC140318 (to OCF). P.P.S.S.A. was supported by the NIH grant 5T32EB016652-02. The authors also thank the Neurobiology Department and the Neurobiology Imaging Facility for consultation and instrument availability that support this work. This facility is supported in part by the Neural Imaging Center as part of an NINDS P30 Core Center (Grant No. NS072030).

Conflict of Interest

O.C.F. declares financial interests in Selecta Biosciences, Tarveda Therapeutics, and Placon Therapeutics.

Keywords

3D cell culture, cell cycle, cellular uptake, nanoparticles, scaffolds

Received: February 5, 2018

Revised: March 1, 2018

Published online: May 8, 2018

- [1] a) D. Peer, J. M. Karp, S. Hong, O. C. Farokhzad, R. Margalit, R. Langer, *Nat. Nanotechnol.* **2007**, *2*, 751; b) E. Blanco, H. Shen, M. Ferrari, *Nat. Biotechnol.* **2015**, *33*, 941.
- [2] a) D. W. Huttmacher, *Nat. Mater.* **2010**, *9*, 90; b) X. Xu, M. C. Farach-Carson, X. Jia, *Biotechnol. Adv.* **2014**, *32*, 1256.
- [3] M. Mahmoudi, *Trends Biotechnol.* **2018**, <https://doi.org/10.1016/j.tibtech.2018.02.014>.
- [4] S. Wilhelm, A. J. Tavares, Q. Dai, S. Ohta, J. Audet, H. F. Dvorak, W. C. Chan, *Nat. Rev. Mater.* **2016**, *1*, 16014.
- [5] a) P. A. Netti, D. A. Berk, M. A. Swartz, A. J. Grodzinsky, R. K. Jain, *Cancer Res.* **2000**, *60*, 2497; b) A. Pluen, Y. Boucher, S. Ramanujan, T. D. McKee, T. Gohongi, E. di Tomaso, E. B. Brown, Y. Izumi, R. B. Campbell, D. A. Berk, R. K. Jain, *Proc. Natl. Acad. Sci. USA* **2001**, *98*, 4628; c) T. T. Goodman, P. L. Olive, S. H. Pun, *Int. J. Nanomed.* **2007**, *2*, 265.
- [6] a) R. G. Thorne, C. Nicholson, *Proc. Natl. Acad. Sci. USA* **2006**, *103*, 5567; b) Y. Mao, J. E. Schwarzbauer, *J. Cell Sci.* **2005**, *118*, 4427.
- [7] E. Panet, T. Mashriki, R. Lahmi, A. Jacob, E. Ozer, M. Vecsler, I. Lazar, A. Tzur, *Nat. Nanotechnol.* **2017**, *12*, 598.
- [8] M. W. Tibbitt, K. S. Anseth, *Biotechnol. Bioeng.* **2009**, *103*, 655.
- [9] a) J. Swift, I. L. Ivanovska, A. Buxboim, T. Harada, P. D. P. Dingal, J. Pinter, J. D. Pajerowski, K. R. Spinler, J.-W. Shin, M. Tewari, *Science* **2013**, *341*, 1240104; b) N. Huebsch, P. R. Arany, A. S. Mao, D. Shvartsman, O. A. Ali, S. A. Bencherif, J. Rivera-Feliciano, D. J. Mooney, *Nat. Mater.* **2010**, *9*, 518; c) S. C. Wei, L. Fattet, J. H. Tsai, Y. Guo, V. H. Pai, H. E. Majeski, A. C. Chen, R. L. Sah, S. S. Taylor, A. J. Engler, *Nat. Cell Biol.* **2015**, *17*, 678.
- [10] J. Alcaraz, R. Xu, H. Mori, C. M. Nelson, R. Mroue, V. A. Spencer, D. Brownfield, D. C. Radisky, C. Bustamante, M. J. Bissell, *EMBO J.* **2008**, *27*, 2829.
- [11] D. T. Butcher, T. Alliston, V. M. Weaver, *Nat. Rev. Cancer* **2009**, *9*, 108.
- [12] a) L. Santos, G. Fuhrmann, M. Juenet, N. Amdursky, C. M. Horejs, P. Campagnolo, M. M. Stevens, *Adv. Healthcare Mater.* **2015**, *4*, 2056; b) L. A. Sawicki, L. H. Choe, K. L. Wiley, K. H. Lee, A. M. Kloxin, *ACS Biomater. Sci. Eng.* **2018**, *4*, 836.
- [13] a) W. Meng, P. Kallinteri, D. Walker, T. Parker, M. C. Garnett, *Exp. Biol. Med.* **2007**, *232*, 1100; b) W. Zhang, Y. Zhang, M. Löbler, K.-P. Schmitz, A. Ahmad, I. Pyykkö, J. Zou, *Int. J. Nanomed.* **2011**, *6*, 535.
- [14] a) S. Huo, H. Ma, K. Huang, J. Liu, T. Wei, S. Jin, J. Zhang, S. He, X.-J. Liang, *Cancer Res.* **2013**, *73*, 319; b) X. Wang, X. Zhen, J. Wang, J. Zhang, W. Wu, X. Jiang, *Biomaterials* **2013**, *34*, 4667; c) H. Gao, J. Qian, Z. Yang, Z. Pang, Z. Xi, S. Cao, Y. Wang, S. Pan, S. Zhang, W. Wang, X. Jiang, Q. Zhang, *Biomaterials* **2012**, *33*, 6264.
- [15] W. Asghar, R. El Assal, H. Shafee, S. Pitteri, R. Paulmurugan, U. Demirci, *Mater. Today* **2015**, *18*, 539.
- [16] a) S. C. Baker, G. Rohman, J. Southgate, N. R. Cameron, *Biomaterials* **2009**, *30*, 1321; b) C. Fischbach, R. Chen, T. Matsumoto, T. Schmelzle, J. S. Brugge, P. J. Polverini, D. J. Mooney, *Nat. Methods* **2007**, *4*, 855; c) E. Santos, R. M. Hernández, J. L. Pedraz, G. Orive, *Trends Biotechnol.* **2012**, *30*, 331.
- [17] a) A. Y. Hsiao, Y. S. Torisawa, Y. C. Tung, S. Sud, R. S. Taichman, K. J. Pienta, S. Takayama, *Biomaterials* **2009**, *30*, 3020; b) T. Liu, B. Lin, J. Qin, *Lab Chip* **2010**, *10*, 1671.

- [18] a) J. S. Jeon, S. Bersini, M. Gilardi, G. Dubini, J. L. Charest, M. Moretti, R. D. Kamm, *Proc. Natl. Acad. Sci. USA* **2015**, *112*, 214; b) B. Kwak, A. Ozcelikkale, C. S. Shin, K. Park, B. Han, *J. Controlled Release* **2014**, *194*, 157; c) P. Agarwal, H. Wang, M. Sun, J. Xu, S. Zhao, Z. Liu, K. J. Gooch, Y. Zhao, X. Lu, X. He, *ACS Nano* **2017**, *11*, 6691.
- [19] a) K. H. K. Wong, J. M. Chan, R. D. Kamm, J. Tien, *Annu. Rev. Biomed. Eng.* **2012**, *14*, 205; b) Z. Liu, X. Han, L. Qin, *Adv. Healthcare Mater.* **2016**, *5*, 871.
- [20] a) X. Gao, Y. Cui, R. M. Levenson, L. W. Chung, S. Nie, *Nat. Biotechnol.* **2004**, *22*, 969; b) P. Desplats, H.-J. Lee, E.-J. Bae, C. Patrick, E. Rockenstein, L. Crews, B. Spencer, E. Masliah, S.-J. Lee, *Proc. Natl. Acad. Sci. USA* **2009**, *106*, 13010.
- [21] B.-M. Ahn, J. Kim, L. Ian, K.-H. Rha, H.-J. Kim, *Urology* **2010**, *76*, 1007.
- [22] K. Wei, V. Serpooshan, C. Hurtado, M. Diez-Cuñado, M. Zhao, S. Maruyama, W. Zhu, G. Fajardo, M. Nosedá, K. Nakamura, *Nature* **2015**, *525*, 479.
- [23] J. A. Kim, C. Åberg, A. Salvati, K. A. Dawson, *Nat. Nanotechnol.* **2012**, *7*, 62.
- [24] E. C. Cho, Q. Zhang, Y. Xia, *Nat. Nanotechnol.* **2011**, *6*, 385.
- [25] L. W. Zhang, N. A. Monteiro-Riviere, *Toxicol. Sci.* **2009**, *110*, 138.
- [26] M. Noh, T. Kim, H. Lee, C.-K. Kim, S.-W. Joo, K. Lee, *Colloids Surf., A* **2010**, *359*, 39.
- [27] S. Behzadi, V. Serpooshan, W. Tao, M. A. Hamaly, M. Y. Alkawareek, E. C. Dreaden, D. Brown, A. M. Alkilany, O. C. Farokhzad, M. Mahmoudi, *Chem. Soc. Rev.* **2017**, *46*, 4218.
- [28] D. Vercauteren, R. E. Vandenbroucke, A. T. Jones, J. Rejman, J. Demeester, S. C. De Smedt, N. N. Sanders, K. Braeckmans, *Mol. Ther.* **2010**, *18*, 561.
- [29] A. I. Ivanov, *Methods Mol. Biol.* **2008**, *440*, 15.
- [30] R. Hardman, *Environ. Health Perspect.* **2006**, *114*, 165.
- [31] S. Laurent, C. Burtea, C. Thirifays, U. O. Häfeli, M. Mahmoudi, *PLoS One* **2012**, *7*, e29997.